

## EPR Studies of the Generation, Structure, and Reactivity of N-Heterocyclic Carbene Borane Radicals

John C. Walton,<sup>\*,†</sup> Malika Makhoulouf Brahmi,<sup>‡</sup> Louis Fensterbank,<sup>‡</sup>  
Emmanuel Lacôte,<sup>\*,‡</sup> Max Malacria,<sup>‡</sup> Qianli Chu,<sup>§</sup> Shau-Hua Ueng,<sup>§</sup>  
Andrey Solovveyev,<sup>§</sup> and Dennis P. Curran<sup>\*,§</sup>

*School of Chemistry, EaStChem, University of St. Andrews, St. Andrews, Fife KY16 9ST, United Kingdom, UPMC University Paris 06, Institut parisien de chimie moléculaire (UMR 7201), C. 229, 4 place Jussieu, 75005 Paris, France, Department of Chemistry, University of Pittsburgh, Pittsburgh, Pennsylvania 15260*

Received November 9, 2009; E-mail: jcw@st-andrews.ac.uk; emmanuel.lacote@upmc.fr; curran@pitt.edu

**Abstract:** N-Heterocyclic carbene boranes (NHC–boranes) are a new “clean” class of reagents suitable for reductive radical chain transformations. Their structures are well suited for their reactivity to be tuned by inclusion of different NHC ring units and by appropriate placement of diverse substituents. EPR spectra were obtained for the boron-centered radicals generated on removal of one of the BH<sub>3</sub> hydrogen atoms. This spectroscopic data, coupled with DFT computations, demonstrated that the NHC–BH<sub>2</sub>• radicals are planar  $\pi$ -delocalized species. *tert*-Butoxyl radicals abstracted hydrogen atoms from NHC–boranes more than 3 orders of magnitude faster than did C-centered radicals, although the rate decreased markedly for sterically shielded NHC–BH<sub>3</sub> centers. Combinations of two NHC–boryl radicals afforded 1,2-bis-NHC–diboranes at rates which also depended strongly on steric shielding. The termination rate increased to the diffusion-controlled limit for sterically unhindered NHC–boryls. Bromine atoms were rapidly transferred to imidazole-based NHC–boryl radicals from alkyl, allyl, and benzyl bromides. Chlorine-atom abstraction was, however, much less efficient and only observed for sterically unhindered NHC–boryls reacting with allylic and benzylic chlorides. For an NHC–borane containing a bulky *thexyl* substituent at boron, the tertiary H atom of the *thexyl* group was selectively removed. The resulting  $\beta$ -boron-containing alkyl radical rapidly underwent  $\beta$  scission of the B–C bond with production of an NHC–boryl radical and an alkene.

### Introduction

Group 14 metal hydrides, especially tin<sup>1</sup> and silicon hydrides,<sup>2</sup> have proved to be very useful reagents for reductive chain transformations of a variety of organic compounds. Efforts to enlarge the scope of such reductions, and decrease their environmental impact,<sup>3</sup> have steered research toward analogous reactions of Group 13 metal hydrides. For example, it has been shown that HInCl<sub>2</sub> is a mild, chemoselective reagent for reducing aromatic aldehydes and halides,<sup>4</sup> as well as organic azides,<sup>5</sup> and that HGaCl<sub>2</sub> is effective for mediating reductive radical-based

cyclization reactions.<sup>6</sup> Although organoboranes play an important role in delivering carbon radicals in many radical-mediated processes,<sup>7</sup> boranes did not appear to be promising as H-atom donors in radical reductions because of their strong boron–hydrogen bonds.<sup>8</sup> Computations at the CBS-4 level provided large BDEs of 105.5 and 100.3 kcal mol<sup>-1</sup> for H<sub>2</sub>B–H and H<sub>3</sub>BBH<sub>2</sub>–H, respectively.<sup>9</sup>

It has been known for some time, however, that the H atoms of boranes ligated to amines and phosphines are more labile.<sup>10</sup> A wide variety of amine– and phosphine–boryl radicals have been generated by H-atom abstraction from the corresponding ligated boranes and take part in rearrangement, abstraction, and addition reactions.<sup>11</sup> The B–H bonds of alkyl amine–boranes are still strong. Computations indicate  $DH^{\circ}(B-H)$  values of 103 and 101 kcal mol<sup>-1</sup> (MP3/6-31G\*\*) for H<sub>3</sub>NBH<sub>3</sub> and MeNH<sub>2</sub>BH<sub>3</sub>, respectively,<sup>10d</sup> and 101.1 kcal mol<sup>-1</sup> (CBS-4) for

<sup>†</sup> University of St. Andrews.

<sup>‡</sup> UPMC.

<sup>§</sup> University of Pittsburgh.

- (1) (a) In *Radicals in Organic Synthesis*; Renaud, P., Sibi, M. P., Eds.; Wiley-VCH: Weinheim, 2001. (b) In *Radicals in Synthesis*; Gansäuer, A., Ed.; Springer-Verlag: Berlin, 2006; Vols. 263 and 264.
- (2) Chatgililoglu, C. *Organosilanes in Radical Chemistry*; Wiley: Chichester, 2004.
- (3) (a) Baguley, P. A.; Walton, J. C. *Angew. Chem., Int. Ed.* **1998**, *37*, 3072–3082. (b) Studer, A.; Amrein, S. *Synthesis* **2002**, 835–849. (c) Darmency, V.; Renaud, P. *Top. Curr. Chem.* **2006**, *263*, 71–106.
- (4) (a) Inoue, K.; Sawada, A.; Shibata, I.; Baba, A. *Tetrahedron Lett.* **2001**, *42*, 4661–4663. (b) Inoue, K.; Sawada, A.; Shibata, I.; Baba, A. *J. Am. Chem. Soc.* **2002**, *124*, 906–907. (c) Takami, K.; Yorimitsu, H.; Oshima, K. *Org. Lett.* **2002**, *4*, 2993–2995. (d) Takami, K.; Mikami, S.; Yorimitsu, H.; Shinokubo, H.; Oshima, K. *Tetrahedron* **2003**, *59*, 6627–6635.
- (5) Benati, L.; Bencivenni, G.; Leardini, R.; Nanni, D.; Minozzi, M.; Spagnolo, P.; Scialpi, R.; Zanardi, G. *Org. Lett.* **2006**, *8*, 2499–2502.

- (6) (a) Takami, K.; Mikami, S.; Yorimitsu, H.; Shinokubo, H.; Oshima, K. *J. Org. Chem.* **2003**, *68*, 6627–6631. (b) Mikami, S.; Fujita, K.; Nakamura, T.; Yorimitsu, H.; Shinokubo, H.; Matsubara, S.; Oshima, K. *Org. Lett.* **2001**, *3*, 1853–1855.
- (7) Darmency, V.; Renaud, P. In *Radicals in Synthesis I*; Gansäuer, A., Ed.; Springer-Verlag: Berlin, 2006; Vol. 263, pp71–106.
- (8) Ryu, I.; Uehara, S.; Hirao, H.; Fukuyama, T. *Org. Lett.* **2008**, *10*, 1005–1008.
- (9) Rablen, P. R. *J. Am. Chem. Soc.* **1997**, *119*, 8350–8360. See also: Barreto, P. R. P.; Vilela, A. F. A.; Gargano, R. *Int. J. Quantum Chem.* **2005**, *103*, 656–684.

$\text{Me}_3\text{NBH}_3$ .<sup>9</sup> In a recent paper,<sup>12</sup> however, H-atom abstraction from N-heteroaryl–boranes was found to be very fast and the corresponding  $DH^\circ(\text{B–H})$  values were much smaller and in the range 67–77 kcal mol<sup>-1</sup>. Applications of amine–boranes to reductive chain transformations have so far been rather limited.

A theoretical study of a series of donor–acceptor complexes of boron revealed that their B–H BDEs were greatly reduced by complexation of the borane moiety with Lewis bases.<sup>9</sup> This finding led some of us to postulate that NHC's would be very effective partners of boron for this purpose and that the resulting NHC–boranes could be serviceable radical chain reducing agents. This prediction was recently confirmed in that secondary xanthates were indeed reductively deoxygenated by the stable NHC–boranes 1,3-bis(2,6-diisopropylphenyl)imidazol-2-ylidene borane, **1a**, and 2-phenyl-1,2,4-triazol-3-ylidene borane, **7** (Barton–McCombie reaction).<sup>13</sup> Furthermore, we obtained good evidence that the mechanism involved chains propagated by NHC–boryl radicals and suggested that the NHC–BH<sub>2</sub>–H BDE was as low as 88 kcal mol<sup>-1</sup>. A preliminary EPR spectrum of the radical derived from **1a** provided key evidence for the postulated mechanism.<sup>14</sup>

These findings signaled that NHC–boranes could be developed as a unique class of reagents capable of mediating a range of radical processes, possibly including some not accessible to tin and silicon hydrides. The modifiable structures of the NHC's should enable the reactivity and selectivity of the NHC–boranes to be readily tuned for particular purposes. Accordingly, we studied the reactivity of a representative set of NHC–boranes mainly by EPR spectroscopy. We found that H atoms were selectively removed by *tert*-butoxyl radicals in a very rapid process, giving previously unknown NHC–boryl radicals. EPR spectra and DFT calculations provided important structural information about this new class of radicals. The termination and atom-transfer reactions of these boron-centered species were

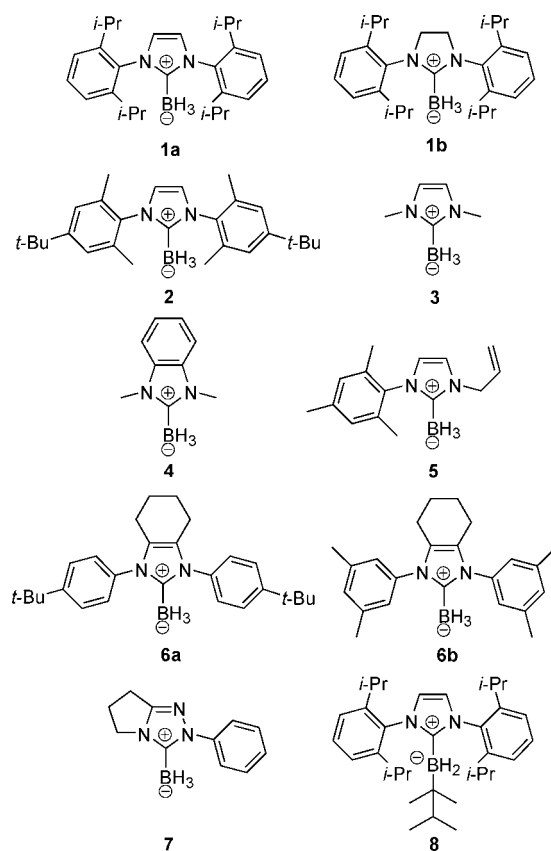


**Figure 1.** Structures of the N-heterocyclic carbene boranes studied. The corresponding NHC–BH<sub>2</sub>• radicals are designated **1a**•, etc.

strongly influenced by steric shielding from substituents pendant from the N atoms of the NHC rings.

## Results and Discussion

**Generation and EPR Spectroscopic Characterization of NHC–Boryl Radicals.** The set of NHC–boranes shown in Figure 1 was chosen to acquaint us with the characteristic reactions of these reagents and to probe the effect of key structural features on their reactivity. A preliminary analysis of the EPR spectrum of the radical **1a**• derived from **1a** has already been communicated.<sup>14</sup> Compounds **1a** and **2–6** are imidazole-based NHC–boranes with 6  $\pi$  electrons in the NHC moiety. This series contains both alkyl and aryl substituents on the N atoms, with consequent variation in the steric shielding around the BH<sub>3</sub> group. In addition, compound **4** has a fused aryl ring in place of the imidazole C=C bond, while **6** has a saturated ring fused to this bond. Compound **1b** was chosen as an example of an imidazolidin-2-ylidene, lacking the 5-center 6-electron  $\pi$  delocalization as a stabilizing factor. Likewise, tetrahydropyrrolo-triazol-3-ylidene **7** was selected to exemplify the reactivity of triazole-based NHC–boranes. The effect of alkyl substituents on the B atom was investigated by means of NHC–*tert*-butylborane **8**.

All these NHC–boranes are air- and moisture-stable white solids that are readily prepared by deprotonation of the corresponding imidazolium or triazolium salt and reaction of the in situ generated NHC with borane. Compounds **1a** and **7** are known,<sup>13</sup> whereas the other complexes are new. Procedures for the preparations and characterization data for all the new complexes are in the Supporting Information.

- (10) (a) Baban, J. A.; Marti, V. P. J.; Roberts, B. P. *J. Chem. Soc., Perkin Trans. 2* **1985**, 1723–1733. (b) Paul, V.; Roberts, B. P. *J. Chem. Soc., Perkin Trans. 2* **1988**, 1183–1193. (c) Baban, J. A.; Roberts, B. P. *J. Chem. Soc., Perkin Trans. 2* **1988**, 1195–1200. (d) Kirwan, N.; Roberts, B. P. *J. Chem. Soc., Perkin Trans. 2* **1989**, 539–550. (e) Dang, H. S.; Roberts, B. P. *Tetrahedron Lett.* **1992**, *33*, 6169–6172. (f) Dang, H. S.; Diart, V.; Roberts, B. P.; Tocher, D. A. *J. Chem. Soc., Perkin Trans. 2* **1994**, 1039–1045. (g) Roberts, B. P.; Steel, A. J. *J. Chem. Soc., Perkin Trans. 2* **1994**, 2411–2422. (h) Lucarini, M.; Pedulli, G. F.; Valgimigli, L. *J. Org. Chem.* **1996**, *61*, 1161–1164. (i) Barton, D. H. R.; Jacob, M. *Tetrahedron Lett.* **1998**, *39*, 1331–1334. (j) Sheeler, B.; Ingold, K. U. *J. Chem. Soc., Perkin Trans. 2* **2001**, 480–486.
- (11) Reviews of amine and phosphine boranes: (a) Carboni, B.; Monnier, L. *Tetrahedron* **1999**, *55*, 1197–1248. (b) Carboni, B.; Carreaux, F. In *Science of Synthesis, Organometallics: Boron Compounds*; Kaufmann, D. E., Matteson, D. S., Eds.; Verlag: Stuttgart, 2004; Vol. 6, pp 455–484. (c) Gaumont, A. C.; Carboni, B. In *Science of Synthesis, Organometallics: Boron Compounds*; Kaufmann, D. E., Matteson, D. S., Eds.; Verlag: Stuttgart, 2004; Vol. 6, pp 485–512.
- (12) (a) Lalevé, J.; Blanchard, N.; Chany, A.-C.; Tehfe, M.-A.; Allonas, X.; Fouassier, J.-P. *J. Phys. Org. Chem.* **2009**, *22*, 986–993. (b) Tehfe, M. A.; Makhlof Brahm, M.; Fouassier, J.-P.; Curran, D. P.; Malacria, M.; Fensterbank, F.; Lacôte, E.; Lalevé, J. Submitted for publication.
- (13) Ueng, S.-H.; Makhlof Brahm, M.; Derat, E.; Fensterbank, L.; Lacôte, E.; Malacria, M.; Curran, D. P. *J. Am. Chem. Soc.* **2008**, *130*, 10082–10083.
- (14) Ueng, S.-H.; Solovvey, A.; Yuan, X.; Geib, S. J.; Fensterbank, L.; Lacôte, E.; Malacria, M.; Newcomb, M.; Walton, J. C.; Curran, D. P. *J. Am. Chem. Soc.* **2009**, *131*, 11256–11262.

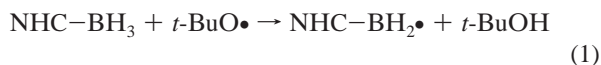
**Table 1.** Experimental and Computed hfs for NHC–Boryl and Related Radicals<sup>a</sup>

NHC–BH <sub>2</sub> • radical	7K or DFT basis set <sup>b</sup>	a(H <sub>α</sub> )G	a( <sup>11</sup> B)G	a(2N) G	a(2H)G	a(other)G
<b>1a</b> •	300	11.4	7.3	4.0	1.0	
<b>1a</b> •	EPR-ii <sup>c</sup>	–10.1	5.1	2.3	–1.0	
<b>2</b> •	270	11.4	7.6	4.0	1.1	
model A ( <b>9</b> •) <sup>d</sup>	EPR-iii	–10.0	5.3	3.1	–1.2	<sup>e</sup>
<b>3</b> •	245	12.0	6.7	4.1	1.2	2.5(6H)
<b>3</b> •	EPR-iii	–10.2	5.2	2.3	–2.0	2.8(6H)
<b>4</b> •	EPR-iii	–7.8	2.8	2.0		–2.5, –1.2, 3.3(6H)
<b>1b</b> •	295	10.4	6.4	4.3		1.2(4H)
model B <sup>f</sup>	EPR-iii	–7.5	2.7	2.2		3.8(4H)
<b>7</b> •	EPR-iii	–8.6, –8.4	4.0	4.3, 1.0		a(N) = 1.4 <sup>g</sup>
NHC–Mes <sub>2</sub> B• <sup>h</sup>	293		7.9	3.0	0.7	2.8(6H)
Me <sub>3</sub> N–BH <sub>2</sub> • <sup>i</sup>	280	9.6	51.3	1.4(1N)		1.4(9H)

<sup>a</sup> All NHC–BH<sub>2</sub>• *g* factors = 2.0028 ± 0.0005. Note that only the magnitudes and not the signs of hfs can be derived from the EPR spectra. <sup>b</sup> DFT computations with the B3LYP functional: geometries optimized with the 6-31G(d) basis set. <sup>c</sup> Computations with the EPR-iii basis set failed. <sup>d</sup> *N,N'*-Diphenylimidazol-2-ylidene–BH<sub>2</sub>•. <sup>e</sup> hfs of Ph-ring H atoms all < ±0.2 G. <sup>f</sup> *N,N'*-Diphenyl-4,5-dihydroimidazol-2-ylidene–BH<sub>2</sub>•. <sup>g</sup> *a*(1H) = 4.3, 2.7, –1.8, and –1.1. *a*(2H<sub>α</sub>) = –2.0. *a*(2H<sub>β</sub>) = 0.7. *a*(H<sub>p</sub>) = –1.7 G. <sup>h</sup> 1,3-Dimethylimidazol-2-ylidene–B(•)Mes<sub>2</sub>; data from Matsumoto et al. <sup>17</sup> <sup>i</sup> Data from Paul et al. <sup>18</sup>

Di-*tert*-butyl peroxide (DTBP) is a convenient photochemical source of *tert*-butoxyl radicals, which are very efficient abstractors of H atoms and are EPR “silent”. Deaerated solutions of individual NHC–boranes and DTBP in *tert*-butylbenzene solvent were irradiated in the resonant cavity of a 9 GHz EPR spectrometer in the expectation that the initial *t*-BuO• radicals would abstract hydrogen from the BH<sub>3</sub> groups of the substrates, thus generating the NHC–boryl radicals. Strong, well-resolved spectra of the corresponding NHC–BH<sub>2</sub>• radicals were obtained from **1a** and **1b**, while **2** and **3** gave somewhat weaker signals. All the spectra were satisfactorily simulated using the Bruker SimFonia and NIEHS WinSim software,<sup>15</sup> and the resulting hyperfine splittings (hfs) are listed in Table 1. The actual and simulated spectra obtained from **2** are shown in Figure 2, and the other spectra are in the Supporting Information.

The hyperfine splittings are entirely appropriate for NHC–boryl radicals, and comparisons with the DFT-computed values for individual NHC–BH<sub>2</sub>• radicals (Table 1) provide further support for the radicals' identities.<sup>16</sup> Furthermore, good correspondence between our hfs and those of the 1,3-dimethylimidazol-2-ylidene-BMes<sub>2</sub> radical, obtained by Matsumoto et al. by reduction of the corresponding cation,<sup>17</sup> was also observed (Table 1). Thus, *t*-BuO• radicals efficiently abstracted H atoms from a variety of NHC–boranes to generate NHC–BH<sub>2</sub>• radicals.



With NHC–borane **4**, an extremely weak EPR spectrum showing only a few central lines was observed. The DFT computations indicated that interaction of the unpaired electron

with all the magnetic nuclei of the BH<sub>2</sub> group, the N–CH<sub>3</sub> groups and aromatic H atoms should be significant (Table 1), thus giving rise to a maximum of 3780 resonance lines. In view of the complex fine structure, it is not surprising that most of the spectral lines of this NHC–boryl radical and of the radicals derived from **5** and **7** are not visible above the noise level. The DFT-computed parameters for **4**• and **7**• are included in Table 1. Hydrogen-atom abstraction from imidazolidin-2-ylidene **1b**, lacking the 5-center 6-electron  $\pi$  delocalization, also took place efficiently, and the hfs of the radical were only slightly smaller in magnitude than those of **1a**•.

It was important to establish if NHC–BH<sub>2</sub>• radicals could be generated in sufficient quantity for EPR spectroscopic detection when *t*-BuO• was replaced by a C-centered radical. We prepared a solution of **1a** and dilauroyl peroxide as the source of undecyl radicals. However, only the undecyl radical [*a*(2H<sub>α</sub>) = 21.8, *a*(2H<sub>β</sub>) = 27.5 G] was observed by EPR spectroscopy on UV photolysis in the temperature range 300–340 K. Even with the sterically much less hindered NHC–borane **3**, no NHC–BH<sub>2</sub>• radicals were detected but only undecyl radicals. It is evident that H-atom abstraction from NHC–BH<sub>3</sub> by *t*-BuO• is much faster than abstraction by *n*-alkyl radicals. This accords well with the measured rate constant [4 × 10<sup>4</sup> M<sup>–1</sup> s<sup>–1</sup> at 301 K] for H-atom abstraction from **1a** by a *sec*-alkyl radical.<sup>14</sup>

The EPR spectra of amine–boryl radicals such as Me<sub>3</sub>N–BH<sub>2</sub>• (and phosphine–boryl radicals) showed them to be  $\sigma$ -type radicals, pyramidal at boron.<sup>10d,18</sup> Comparison with the hfs of the radicals from **1a**, **2**, and **3** shows NHC–BH<sub>2</sub>• radicals have much smaller *a*(<sup>11</sup>B) and larger *a*(N) than Me<sub>3</sub>N–BH<sub>2</sub>• (Table 1). This indicates that the NHC–BH<sub>2</sub>• radicals are roughly planar at boron and that the unpaired electron is delocalized into the NHC ring. The structures of the NHC–boryl radicals and their SOMOs were computed by DFT employing the B3LYP functional.<sup>19</sup> The structures of model A [*N,N'*-diphenylimidazol-2-ylidene–BH<sub>2</sub>• (**9**•)] and benzimidazole-derived radical **4**•, optimized with the 6-31G(d) basis set, and their associated SOMOs are shown in Figure 3.

The whole imidazole–BH<sub>2</sub> unit in **9**• and the benzimidazole–BH<sub>2</sub> unit in **4**• were found to be planar, and interestingly, the two Ph rings in **9**• were orthogonal to the NHC moiety and hence out of conjugation. This is in good accord with the absence of resolvable hfs from the aromatic H atoms in the EPR spectra of the radicals **1a**• and **2**•. The C–B bond lengths of 1.498 and 1.500 Å in **9**• and **4**•, respectively, were shorter than the C–B bonds of the corresponding NHC–BH<sub>3</sub> precursors by about 0.1 Å. Concomitantly, the C–N bonds were longer than those of the precursors by about 0.03 Å. These structural changes are analogous to those found for C-centered radicals in comparison with their hydrocarbon precursors.<sup>20</sup> The barrier to internal rotation about the C–BH<sub>2</sub> bond in the radical **3**• was computed to be 19.5 kcal mol<sup>–1</sup>, confirming the partial double-bond character of this bond. The SOMO in **9**• is an essentially pure  $\pi$  system extending over the BH<sub>2</sub> group and the imidazole ring but, as expected from the EPR data, not to the Ph rings. Similarly, in **4**•, the SOMO extends to the whole benzimidazole moiety. The NHC–boryl radicals are quite unlike the bent  $\sigma$ -amine–boryl radicals but quite like the  $\pi$ -delocalized benzyl

(15) Duling, D. R. *J. Magn. Reson. B* **1994**, *104*, 105–110. The minor contributions to the EPR spectra from the <sup>10</sup>B isotopomers were omitted.

(16) The DFT-computed <sup>11</sup>B hfs depended strongly on the basis set varying from 13.6 (6-31G(d) basis set) to 4.9 G (6-311G(d) basis set) (See Table S1 in the Supporting Information).

(17) Matsumoto, T.; Gabbai, F. P. *Organometallics* **2009**, *28*, 4252–4253.

(18) Paul, V.; Roberts, B. P.; Robison, C. A. S. *J. Chem. Res. (S)* **1988**, 264–265.

(19) Frisch, M. J.; et al. *Gaussian 03*, Revision A.1; Gaussian, Inc.: Pittsburgh, PA, 2003.

(20) See, for example: (a) Pacansky, J.; Dupuis, M. *J. Chem. Phys.* **1979**, *71*, 2095–2098. (b) Pacansky, J.; Schubert, W. *J. Chem. Phys.* **1982**, *76*, 1459–1466.



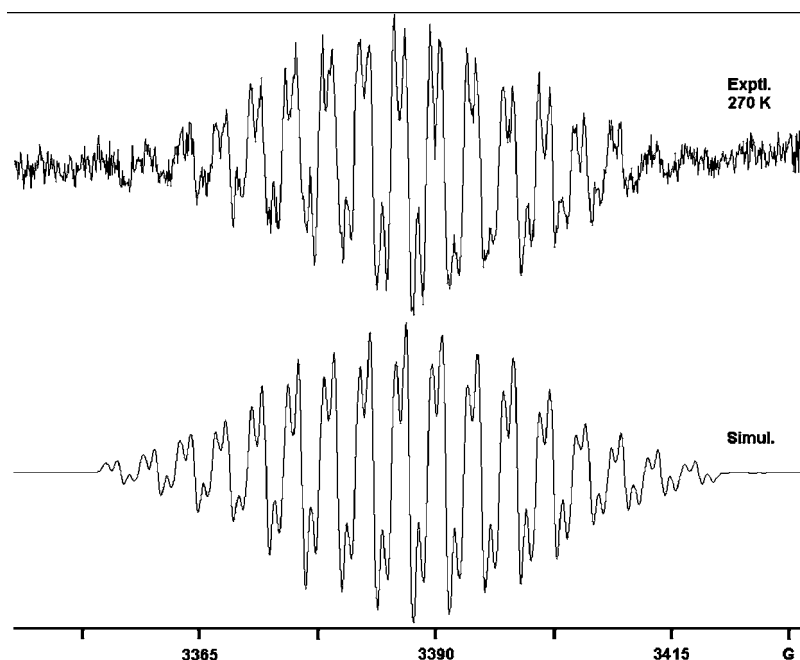


**Figure 2.** EPR (9.5 GHz) spectrum of the NHC–BH<sub>2</sub>• radical **2**•. (Top) First-derivative experimental spectrum at 270 K in *t*-BuPh solution. (Bottom) Computer simulation with parameters noted in Table 1.

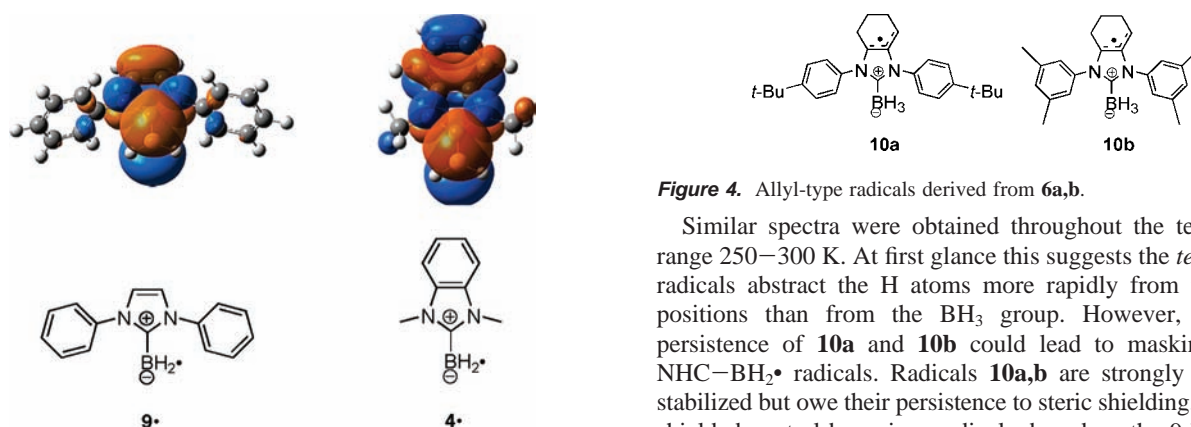


**Figure 3.** DFT-computed structures and SOMOs of NHC–BH<sub>2</sub>• radicals.

radical. Similar delocalized electronic structures are expected for imidazolylidene, triazolylidene, and thiazolylidene NHC–boryl species. Consequently, NHC–boryl radicals should possess significant resonance delocalization, and therefore, they will be thermodynamically stabilized. This will be a major factor in lowering the transition-state energy of H-atom transfer reactions of NHC–boranes.

When a solution of NHC–borane **6a** and DTBP was photolyzed in the EPR cavity, a strong spectrum of a very persistent radical was obtained. The spectrum did not decay in 21 h in the dark, although it degraded in a few minutes if UV photolysis was continued. Analysis and simulation gave the following results:  $a(2H) = 0.91$ ,  $a(2H) = 2.74$ ,  $a(1H) = 9.66$ ,  $a(2H) = 9.75$ ,  $a(1N) = 10.50$  G at 300 K. A similar persistent spectrum having  $a(2H) = 0.94$ ,  $a(2H) = 2.74$ ,  $a(1H) = 10.55$ ,  $a(2H) = 9.68$ ,  $a(1N) = 10.41$ ,  $a(1N) = 0.95$  G at 300 K was obtained from the related cyclohexyl-substituted NHC–borane **6b**. It is evident that these are not NHC–boryl radicals but rather allyl-type radicals **10a,b** derived by abstraction of the allylic H atoms of the cyclohexane rings (Figure 4).

**Figure 4.** Allyl-type radicals derived from **6a,b**.

Similar spectra were obtained throughout the temperature range 250–300 K. At first glance this suggests the *tert*-butoxyl radicals abstract the H atoms more rapidly from the allylic positions than from the BH<sub>3</sub> group. However, the great persistence of **10a** and **10b** could lead to masking of any NHC–BH<sub>2</sub>• radicals. Radicals **10a,b** are strongly resonance stabilized but owe their persistence to steric shielding. Sterically shielded neutral boronium radicals, based on the 9-bora-9,10-dihydroanthracene scaffold with substituted 2,2'-bipyridyl ligands, had significant spin density on boron and were also found to be persistent.<sup>21</sup>

**Combination Reactions of NHC–Boryl Radicals.** The EPR spectrum of the radical from NHC–borane **1a** did not disappear instantly when the UV light was shuttered, suggesting it had some persistence. To learn more about this, samples of **1a** and DTBP in *t*-BuPh were prepared and degassed and the EPR magnetic field was fixed at the maximum intensity of the radical signal. The decay of the signal was then monitored as a function of time on shuttering the UV photolysis beam. Several separate samples were examined, and a typical curve is shown in Figure 5 for the decay at 300 K. The initial concentration of the NHC–BH<sub>2</sub>• radical was determined from the average of the double integrals of the full spectra before and after photolysis. The decay could not be satisfactorily fitted by a first-order plot (see Supporting Information), but good fit was obtained for second-order decay having  $2k_t = 9.0 \times 10^6 \text{ M}^{-1} \text{ s}^{-1}$  (Figure 5).

The decay of this radical was monitored at three lower temperatures, and the best-fit  $2k_t$  values were plotted in

(21) Wood, T. K.; Piers, W. E.; Keay, B. A.; Parvez, M. *Chem. Commun.* **2009**, 5147–5149.

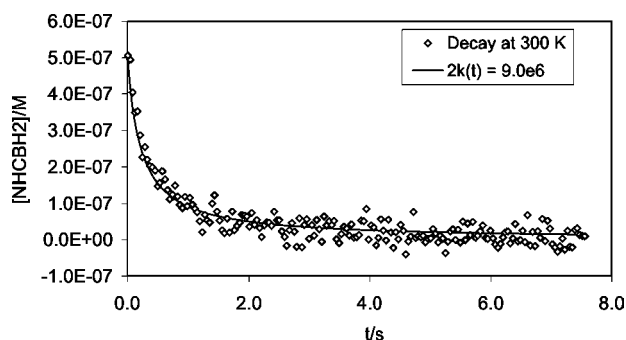


**Figure 5.** Decay of the EPR signal of radical **1a•** as a function of time at 300 K.

**Table 2.** Combination Rate Constants for NHC–Boryl Radicals<sup>a</sup>

radical	T, K	[NHC–BH <sub>2</sub> •] <sub>i</sub> , M <sup>b</sup>	2 <i>k<sub>t</sub></i> , M <sup>-1</sup> s <sup>-1</sup>	steric energy, <sup>c</sup> kcal mol <sup>-1</sup>
<b>1a•</b>	300	5.1 × 10 <sup>-7</sup>	9.0 × 10 <sup>6d</sup>	260.7 [83]
<b>1b•</b>	300	3.1 × 10 <sup>-7</sup>	8.1 × 10 <sup>6</sup>	281.4 [95]
<b>2•</b>	290	7.3 × 10 <sup>-7</sup>	50 × 10 <sup>6</sup>	249.6 [62]
<b>3•</b>	300		~5000 × 10 <sup>6</sup>	74.5 [17]

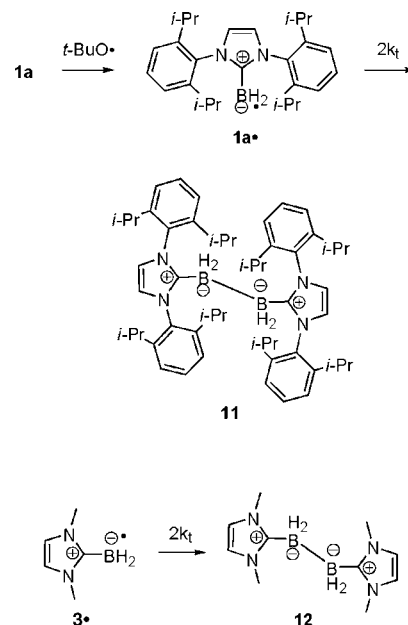
<sup>a</sup> In *t*-BuPh solution. <sup>b</sup> Initial concentration of NHC–BH<sub>2</sub>• radical. <sup>c</sup> Computed by the MM2 method for the B3LYP/6-31G(d) optimum structures: values for MM2-optimized structures in brackets. <sup>d</sup> Arrhenius parameters: log(*A<sub>t</sub>*/M<sup>-1</sup> s<sup>-1</sup>) = 11.9 ± 0.8, *E<sub>t</sub>* = 6.9 ± 0.4 kcal mol<sup>-1</sup>.

Arrhenius form (see Supporting Information). Linearity was good (*R*<sup>2</sup> = 0.991), yielding *E<sub>t</sub>* = 6.9 ± 0.4 kcal mol<sup>-1</sup> and log(*A<sub>t</sub>*/M<sup>-1</sup> s<sup>-1</sup>) = 11.9 ± 0.8. The EPR spectral intensities were poorer for the radicals **1b•** and **2•**; however, second-order decay rate constants were obtained in the same way, at a single temperature, for each radical. The individual resonance lines of the EPR spectrum of radical **3•** were too weak for satisfactory decay curves to be obtained. However, it was apparent that the signal from this radical disappeared the instant the UV light was shuttered. This demonstrated that termination was extremely rapid and comparable to that of small C-centered radicals. It is probable therefore that termination is diffusion controlled or nearly so. The decay rate constants are collected in Table 2, including a typical diffusion rate constant for the radical **3•**.

The decay curves established that terminations were second order in the NHC–BH<sub>2</sub>• radical concentrations. Since disproportionations are not possible for these radicals, their decay processes must be dimerizations leading to the formation of 1,2-bis-NHC–diborane derivatives such as **11** and **12**, Scheme 1. There are literature precedents for the stability of such compounds.<sup>22</sup> In one experiment with **1a** at 300 K, photolysis was prolonged for 30 min so that a significant amount of dimer built up. Subsequent heating of this solution in the dark at 350 K did not lead to any detectable NHC–boryl radical. These observations suggest the dimerization process is not significantly reversible in the accessible temperature range. The absence of curvature in the Arrhenius plot was consistent with this conclusion.

Most small C-centered radicals dimerize (and/or disproportionate) extremely rapidly at the diffusion-controlled limit.<sup>23</sup> For example, the measured 2*k<sub>t</sub>* for benzyl radical dimerization at 300 K in cyclohexane was 4.1 × 10<sup>9</sup> M<sup>-1</sup> s<sup>-1</sup> [log *A<sub>t</sub>*/M<sup>-1</sup> s<sup>-1</sup>

**Scheme 1.** Dimerization of NHC–Boryl Radicals



= 10.7, *E<sub>t</sub>* = 1.94 kcal mol<sup>-1</sup>]<sup>24</sup> and for *t*-Bu• radical termination in *n*-heptane at 294 K 2*k<sub>t</sub>* = 8 × 10<sup>9</sup> [log *A<sub>t</sub>*/M<sup>-1</sup> s<sup>-1</sup> = 11.7, *E<sub>t</sub>* = 2.4 kcal mol<sup>-1</sup>].<sup>23a</sup> The sterically unhindered radical **3•** probably dimerizes at about this rate, but radical **1a•** dimerizes nearly 3 orders of magnitude more slowly and there is a much higher energy barrier for formation of the B–B bond.

The DFT-computed structure for **1a•** and the semiempirical AM1 structure for **11** (Figure 6) give an idea of the substantial steric shielding of the BH<sub>2</sub> group by the 2,6-diisopropylphenyl substituents. The “steric energies”, computed by the empirical MM2 method, for radical structures optimized at the B3LYP/6-31G(d) level are shown in Table 2 for comparison. These SEs indicate that shielding is rather substantial for the radicals from **1a**, **1b**, and **2**. The rough correlation between the SE values and the log 2*k<sub>t</sub>* data suggests that steric shielding is indeed the main factor slowing the combination reactions of the NHC–BH<sub>2</sub>• radicals. The radical **1b•** lacks the imidazole ring conjugation possessed by the other species. Steric shielding of the radical center is about the same as in the radical **1a•**. The fact that the 2*k<sub>t</sub>* values for the radicals derived from **1a** and **1b** are rather similar (Table 2) shows it is steric shielding rather than electronic stabilization that controls the dimerization process.

**Hydrogen Abstraction from NHC–Boranes.** The success of the EPR experiments showed that H-atom abstraction from the NHC–boranes by *tert*-butoxyl radicals was very fast. To measure the rate of this process, a substrate of comparable reactivity toward *t*-BuO• was sought for competition experiments. After some trials, we found that UV irradiation of

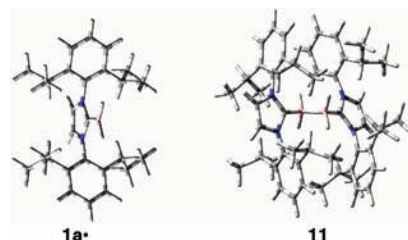


**Figure 6.** Structures of radical **1a•** and dimer **11**.

(22) Wang, Y.; Quillian, B.; Wei, P.; Wannere, C. S.; Xie, Y.; King, R. B.; Schaefer, H. F.; Schleyer, P. V.; Robinson, G. H. *J. Am. Chem. Soc.* **2007**, *129*, 12412–12413.

(23) (a) Schuh, H.-H.; Fischer, H. *Helv. Chim. Acta* **1978**, *61*, 2130–2164. (b) Schuh, H.-H.; Fischer, H. *Int. J. Chem. Kinet.* **1976**, *8*, 341–356.

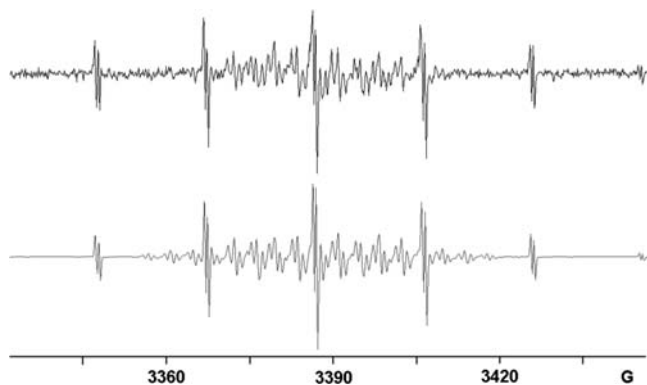
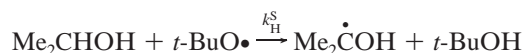
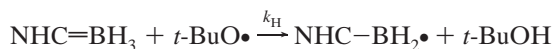


**Figure 7.** EPR spectrum showing **1a•** and  $\text{Me}_2\text{C}(\bullet)\text{OH}$  from photoreaction of **1a** and propan-2-ol with DTBP. (Top) Experimental spectrum in *t*-BuPh at 295 K. (Bottom) Computer simulation.

solutions containing an NHC–borane and propan-2-ol together with DTBP gave rise to EPR spectra showing *both* the NHC–boryl radical and the 2-hydroxypropan-2-yl radical. Stock solutions of known concentrations of NHC–boranes **1a**, **2**, and **3** together with DTBP were prepared. To each was added known amounts of propan-2-ol, and the EPR spectra were recorded during photolysis. Figure 7 shows the spectra of the mixture of **1a•** and  $\text{Me}_2\text{C}(\bullet)\text{OH}$  obtained from the reaction with **1a** and propan-2-ol. The ratio of the concentrations of the two radicals was obtained from spectral simulations. For each NHC–borane, spectra were obtained with three different concentrations of propan-2-ol and the results were averaged.



It can easily be shown that

$$k_{\text{H}}/k_{\text{H}}^{\text{S}} = [\text{NHC}-\text{BH}_2\bullet][i\text{-PrOH}]/[\text{Me}_2\text{C}(\bullet)\text{OH}][\text{NHC}-\text{BH}_3] \quad (2)$$

provided the termination rates of the two radicals are the same. The average values of the concentration ratios are listed in Table 3 along with data for some related H-atom abstractions. The rate constant for H-atom abstraction from  $\text{Me}_2\text{CHOH}$  is known to be  $1.8 \times 10^6 \text{ M}^{-1} \text{ s}^{-1}$  at 295 K,<sup>25</sup> and hence,  $k_{\text{H}}$  values can be derived for the three NHC–boranes. However, as shown above, the  $2k_{\text{t}}$  values for the sterically congested NHC– $\text{BH}_2\bullet$  radicals from **1a** and **2** are considerably smaller than  $2k_{\text{t}}$  for the  $\text{Me}_2\text{C}(\bullet)\text{OH}$  radical, which is known to be ca.  $4 \times 10^9 \text{ M}^{-1} \text{ s}^{-1}$  at 300 K in hydrocarbon solvents.<sup>26</sup> The measured ratios will, therefore, lead only to upper limits for the corresponding  $k_{\text{H}}$  values.

- (24) Lezni, M.; Schuh, H.; Fischer, H. *Int. J. Chem. Kinet.* **1979**, *11*, 705–713.  
 (25) (a) Paul, H.; Small, R. D.; Scaiano, J. C. *J. Am. Chem. Soc.* **1978**, *100*, 4520–4527. (b) Malatesta, V.; Scaiano, J. C. *J. Org. Chem.* **1982**, *47*, 1455–1459.  
 (26) Griller, D. Radical Reaction Rates in Liquids. In *Landolt-Börnstein: Numerical Data and Functional Relationships in Science and Technology*; Fischer, H., Ed.; Springer-Verlag: Berlin, 1984; Vol. 13a, pp 5–130.  
 (27) Effio, A.; Griller, D.; Ingold, K. U.; Scaiano, J. C.; Sheng, S. J. *J. Am. Chem. Soc.* **1980**, *102*, 6063–6068.  
 (28) Newcomb, M.; Park, S. U. *J. Am. Chem. Soc.* **1986**, *108*, 4132–4134.

**Table 3.** Rate Constants for H-Atom Abstraction from NHC–Boranes and Related Molecules<sup>a</sup>

radical	substrate	BDE, kcal mol <sup>-1</sup>	$\frac{[\text{NHC}-\text{BH}_2\bullet][i\text{-PrOH}]}{[\text{Me}_2\text{C}(\bullet)\text{OH}][\text{NHC}-\text{BH}_3]}$	$k_{\text{H}}$ , M <sup>-1</sup> s <sup>-1</sup>	ref
$\text{R}_2\text{CH}\bullet$ <sup>b</sup>	<b>1a</b>	88		$4 \times 10^4$	14
<i>t</i> -BuO•	<b>1a</b>	88	82	$\leq 1.4 \times 10^8$	this work
<i>t</i> -BuO•	<b>2</b>		456	$\leq 8.2 \times 10^8$	this work
<i>t</i> -BuO•	<b>3</b>		1440	$2.6 \times 10^9$	this work
<i>t</i> -BuO•	1,4-CHD <sup>c</sup>	76		$5.4 \times 10^7$	25a, 27
$\text{RCH}_2\bullet$	1,4-CHD <sup>c</sup>	76		$2 \times 10^5$	28
<i>t</i> -BuO•	$\text{Bu}_3\text{SnH}$	78		$2.2 \times 10^9$	29
$\text{RCH}_2\bullet$	$\text{Bu}_3\text{SnH}$	78		$2.4 \times 10^6$	30

<sup>a</sup> Solution data at 295 K. <sup>b</sup> 1-Cyclobutyl-dodecyl radical. <sup>c</sup> 1,4-Cyclohexadiene.

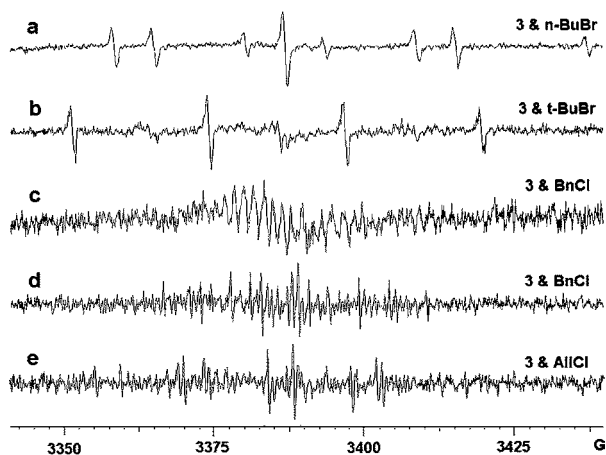
Nonetheless, these upper limits may not be very different from the actual rate constants because rapid cross-termination with *t*-BuO• radicals may predominate. In parallel work on the use of NHC–boranes as co-initiators in radical polymerizations, Lalevée and co-workers used time-resolved laser flash photolysis experiments to measure  $k_{\text{H}} = 9.5 \times 10^7 \text{ M}^{-1} \text{ s}^{-1}$  for the reaction of *t*-BuO• with **1a** at 300 K.<sup>12b</sup> This compares favorably with the upper limit measured by EPR experiments,  $k_{\text{H}} \leq 1.4 \times 10^8 \text{ M}^{-1} \text{ s}^{-1}$  (Table 3, second entry). For radical **3•**, derived from the unhindered NHC–borane **3**, the termination rate constants of the two radicals will be equal to within the experimental error so the derived  $k_{\text{H}}$  will be reliable.

Table 3 shows the  $k_{\text{H}}$  values for the *t*-BuO• radical increase in magnitude for the NHC– $\text{BH}_3$  substrates from **1a** to **2** to **3**, and this is in line with the decrease in steric shielding of the  $\text{BH}_3$  group along this series. The magnitude of  $k_{\text{H}}$  for *t*-BuO• with **3** is comparable to that of the same radical with  $\text{Bu}_3\text{SnH}$ . These reactions are extremely fast, and H-atom abstraction occurs on almost every encounter of the reactants in solution. For abstraction from the NHC–borane **1a**, the increased magnitude of  $k_{\text{H}}$  for the *t*-BuO• radical, as compared with the C-centered radical, is particularly striking. The data for other substrates show that  $k_{\text{H}}$  values are always greater for *t*-BuO• but by smaller factors. The BDE for  $\text{Bu}_3\text{SnH}$  is 10 kcal mol<sup>-1</sup> less than that of **1a**. It is not surprising therefore that  $k_{\text{H}}(\mathbf{1a})$  for a C-centered radical is nearly 2 orders of magnitude slower than  $k_{\text{H}}(\text{Bu}_3\text{SnH})$  for a C-centered radical (Table 3). However, the fact that  $k_{\text{H}}$  for *t*-BuO• with **3** is comparable to that of the same radical with  $\text{Bu}_3\text{SnH}$  suggests the H abstraction by *t*-BuO• is not simply controlled by the thermochemistry but that other factors must play a part.

**Halogen-Atom Abstraction by NHC–Boryl Radicals.** Group 14 metal-centered radicals readily abstract halogen atoms from alkyl halides. We therefore investigated the propensity of NHC–boryl radicals to abstract halogen atoms by generating them in the presence of various organic halides and then scrutinizing the EPR spectra. Known quantities of various alkyl halides (usually 10  $\mu\text{L}$ ) were added to aliquots (0.2 mL) from a stock solution of **3** (ca. 0.1 mM) and DTBP in *tert*-butylbenzene. During UV photolyses at 300 K the EPR spectra shown in Figure 8 were obtained.

Good quality spectra of the corresponding *n*- and *tert*-butyl radicals were observed during UV photolyses with added

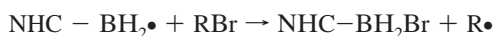
- (29) Scaiano, J. C. *J. Am. Chem. Soc.* **1980**, *102*, 5399–5400.  
 (30) Chatgililoglu, C.; Ingold, K. U.; Scaiano, J. C. *J. Am. Chem. Soc.* **1981**, *103*, 7739–7742.  
 (31) Most of the EPR spectra were recorded with 2.0 mW power and 1.0  $G_{\text{pp}}$  modulation intensity. However, for detection of the easily saturated benzyl radical 1.0 mW power and 0.2  $G_{\text{pp}}$  modulation intensity was needed.



**Figure 8.** EPR spectra obtained from UV photolyses of solutions of **3** and DTBP with various alkyl halides at 300 K: (a) with added *n*-BuBr showing part of the *n*-Bu• radical spectrum, (b) with added *t*-BuBr showing part of the *t*-Bu• radical spectrum, (c) with added PhCH<sub>2</sub>Cl showing the NHC–BH<sub>2</sub>• radical **3**•, (d) same sample as c but with low power and smaller modulation intensity,<sup>31</sup> showing the benzyl radical, (e) with added allyl chloride showing the allyl radical.

1-bromobutane and 2-bromo-2-methylpropane, respectively (Figure 8a and 8b), showing that boron-centered radical **3**• readily abstracted *primary* and *tertiary* bromine atoms at room temperature. With added Me<sub>3</sub>CCl, however, only radical **3**• was detectable, indicating that chlorine-atom abstraction was too slow for spectroscopic observation. With PhCH<sub>2</sub>Cl as substrate, we initially observed only the NHC–boryl radical **3**• (Figure 8c), but on reducing the microwave power and modulation intensity,<sup>31</sup> a new spectrum appeared with hfs identical to those of the benzyl radical. In fact, a mixture of **3**• and PhCH<sub>2</sub>• actually resulted. Thus, radical **3**• *did* abstract Cl atoms from benzyl chloride to give the resonance-stabilized benzyl radical, although the process was comparatively slow. Similarly, a weak spectrum of the allyl radical was observed with allyl chloride as substrate (Figure 8e).

Similar experiments were carried out with NHC–boranes **1a**, **2–5**, and **7**, and good spectra of alkyl radicals were observed in every case with an alkyl bromide as a reaction partner, even for precursors **4**, **5**, and **7** where the initial NHC–BH<sub>2</sub>• radicals had not been detected. With **1b** as reactant the spectra showed a mixture of the NHC–BH<sub>2</sub>• radical with minor amounts of the *tert*-butyl and a trace of the *n*-butyl radical with *tert*- and *n*-alkyl bromide coreactants, respectively. Chlorine-atom abstraction was only detected, however, with the sterically unhindered radical **3**•.



R = primary-alkyl, *tert*-alkyl, benzyl, allyl

The relative intensities of the released alkyl radicals are recorded in Table 4. The initial reactant concentrations and reaction conditions were essentially the same for all these experiments, so the relative intensities are related to the overall efficiency of the abstraction. However, the relative intensities will depend on the rates of termination reactions as well as on the rates of bromine-atom abstraction. Column 3 of Table 4 shows that the *n*-Bu• radical intensity increased as the steric shielding of the NHC–boryl radical center decreased on going from **1a** to **2** to **3** as might be expected. Surprisingly, however, the reverse was the case for the *t*-Bu• radical. Possibly this is a consequence of

**Table 4.** Relative EPR Signal Intensities in Reactions of NHC–BH<sub>2</sub>• Radicals with 1-Bromobutane and 2-Bromo-2-methylpropane<sup>a</sup>

precursor NHC–BH <sub>2</sub>	<i>t</i> -Bu• relative EPR intensity	<i>n</i> -Bu• relative EPR intensity
<b>1a</b>	2.2	0.6
<b>2</b>	1.6	1.6
<b>3</b>	1.0	3.4
<b>4</b>	0.3	n.d.
<b>5</b>	0.4	n.d.
<b>1b</b>	0.4	≤0.1
<b>7</b>	0.2	n.d.

<sup>a</sup> Determined from the double integrals of the EPR spectra relative to the *t*-Bu• intensity with **3**; n.d. = not determined.

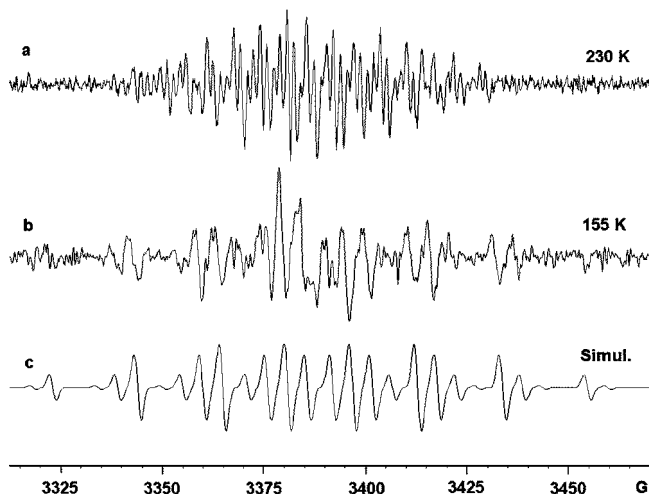


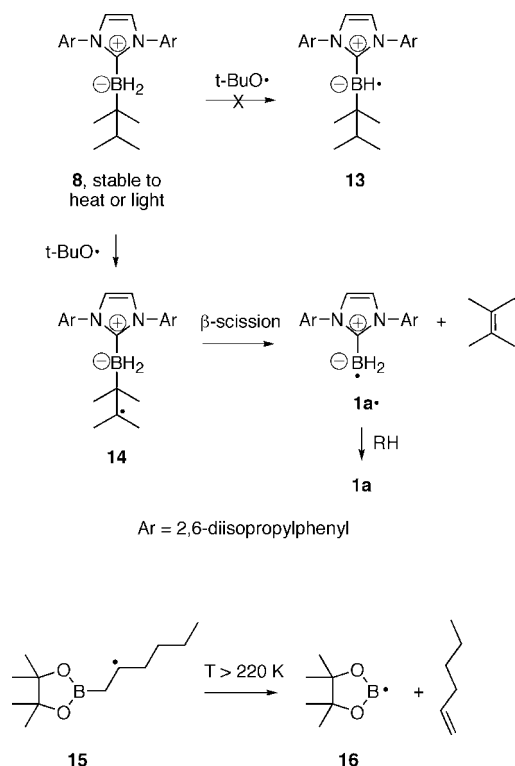
**Figure 9.** EPR spectra on treatment of **8** with *tert*-butoxyl radicals. (a) Radical **1a**• at 230 K in *t*-BuPh solution. (b) Spectrum at 155 K in cyclopropane solution. (c) Computer simulation of radical **14**.

slower cross-combination of the *t*-Bu• radical with the sterically congested NHC–boryl radical **1a**•. The imidazole-based reagents with 6  $\pi$ -electron delocalization were more efficient than the others.

Bromine-atom abstraction was least efficient with the imidazolidin-2-ylidene-based radical **1b**• and the triazole-based radical **7**•. The imidazolidine-containing radical lacks the quasi-aromatic structure but has similar steric shielding to **1a**• and a similar termination rate. Thus, the much slower bromine-atom transfer rate is due to electronic effects. The smaller hfs on boron and on the  $\alpha$ -H atoms (Table 1) indicate lower unpaired spin on boron for the imidazolidine-containing radical **1b**•, and this is consistent with a slower rate of bromine-atom abstraction. Experimental hfs were not obtained for the triazole-based radical **7**•, but the computed hfs (Table 1) predict lower unpaired spin on boron for this system too. It is clear that NHC–borane **3** should be a useful reagent for reductive transformations of a wide range of alkyl bromides but will probably only reduce allyl, benzyl, and similarly activated chlorides.

**Elimination Reaction of the NHC Thexyl–Borane 8.** The thexyl–borane **8** was examined as an example of an NHC–borane with alkyl substitution at boron. UV photolysis of a solution containing **8** and DTBP in *t*-BuPh gave rise to a good spectrum of an NHC–boryl radical (Figure 9a). Surprisingly, this was not the NHC–BH(•)thexyl radical **13**. Inspection and simulation showed this to be radical **1a**• identical to that obtained from **1a**. To check if the boron–carbon bond simply underwent homolytic scission, a solution of **8** in *t*-BuPh, without added



Scheme 2. Radical Reaction of **8**

DTBP, was heated up to 360 K in the EPR cavity. No significant signals were observed. Similarly, on heating up to 360 K, with simultaneous UV irradiation, no EPR signals were observed. Direct homolysis of the B–C bond was not therefore detectable in the accessible temperature range.

The most likely explanation seemed to be that the *tert*-butoxyl radicals were abstracting the tertiary H atom from the branched thexyl group in preference to the BH<sub>3</sub> group. This is not too surprising given the additional steric shielding of the boron center compared to **1a**. The resulting C-centered radical **14** subsequently underwent  $\beta$  scission to release the NHC–BH<sub>2</sub>• radical **1a**• and 2,3-dimethylbut-2-ene (Scheme 2). If this were correct, we reasoned that the unrearranged C-centered radical **14** might be spectroscopically observable at lower temperatures. Accordingly, a sample of **8** (3.3 mg) with DTBP (ca. 0.02 mL) in cyclopropane (ca. 0.3 mL) was prepared on a vacuum line and then UV irradiated at several temperatures in the EPR cavity. At 180 K the spectrum showed a mixture of radical **1a**• and a new radical, and at 155 K (Figure 9b) this new radical predominated.

The new radical was satisfactorily simulated with the following EPR parameters:  $a(6\text{H}) = 20.8$  G,  $a(^{11}\text{B}) = 16.0$  G (Figure 9c).<sup>32</sup> These parameters are about what would be expected for the C-centered radical **14**. For comparison, the EPR spectrum of the 2-(tetramethyldioxaborolane)ethyl radical **15**, which also contains a  $\beta$ -boron atom, was found to have fairly similar hfs [ $a(\text{H}_\alpha) = 22.1$ ,  $a(^{11}\text{B}_\beta) = 17.7$ ,  $a(2\text{H}_\beta) = 22.1$ ,  $a(2\text{H}_\beta)$

$= 27.0$  G at 180 K].<sup>33</sup> Additional evidence supporting the  $\beta$ -scission process of Scheme 2 was obtained by GC-MS analysis of the products from a 2 h UV photolysis of a solution of **8** in DTBP at rt. The main products were shown from their mass spectra to be Me<sub>2</sub>C–CMe<sub>2</sub> and **1a** together with products derived from the DTBP (ethane, acetone, *tert*-butanol, etc.).

The EPR spectra were too weak for radical concentration measurements, but we estimated by visual inspection and simulation that radicals **14** and **1a**• were of equal concentration at about  $T_{\text{mid}} = 180$  K. The activation energies  $E_r$  of many unimolecular reactions correlate with EPR-derived  $T_{\text{mid}}$  values according to<sup>34</sup>

$$E_r/\text{kcal mol}^{-1} = 0.044T_{\text{mid}} + 0.22 \quad (3)$$

Strictly, this linear correlation is only expected to hold for processes in which the rearranged and unrearranged radicals terminate at the diffusion-controlled limit. In the case of radical **14** the ejected radical **1a**• terminates more slowly than this, so only a lower limit for  $E_r$  will be obtained. Use of eq 3 leads to  $E_r \geq \text{ca. } 8$  kcal mol<sup>-1</sup>, and for a normal pre-exponential factor of 10<sup>13</sup> s<sup>-1</sup>, the rate constant for the  $\beta$  scission of **14** at 300 K will be  $\leq \text{ca. } 10^7$  s<sup>-1</sup>. We can conclude that  $\beta$  scission of **14** is a fast process, and this is consistent with the resonance stabilization of the released NHC–boryl radical **1a**• and the comparative stability of the tetrasubstituted alkene. It also corresponds well with the idea<sup>35</sup> that NHC complexation weakens boron–carbon bonds as well as boron–hydrogen bonds.  $\beta$  Scission was also reported for the only other known  $\beta$ -boron-containing radical **15** (and one analog),<sup>33</sup> and of course,  $\beta$  scissions are rapid for L<sub>n</sub>MCH<sub>2</sub>CH<sub>2</sub>• radicals, where M = second and subsequent row element.

## Conclusions

NHC–boryls are a new class of boron-centered radicals, and an understanding of their structures and reactions is beginning to emerge from these EPR and complementary laser flash photolysis studies,<sup>12b</sup> both supplemented by calculations. NHC–boryl radicals can readily be generated by selective H-atom abstraction by *t*-BuO• radicals from “clean” precursor NHC–boranes with long shelf lives. A good range of NHC–ring structures and substituent patterns are available, enabling the electronic and steric properties to be tuned. Imidazole-based NHC–boranes having 4,5-alkyl substituents were an exception in that allylic H-atom abstraction competed, thus generating long-lived allyl-type radicals rather than the desired NHC–boryls. The EPR hfs indicated that the NHC–BH<sub>2</sub>• radicals had planar structures in which the unpaired electron was contained in a  $\pi$ -orbital delocalized round the whole system. They differed markedly therefore from amine- and phosphine–boryls, the only other well-investigated class of boron-centered radicals, which are  $\sigma$ -type species pyramidal at boron.

*tert*-Butoxyl radicals abstracted hydrogen atoms from NHC–boranes more than 3 orders of magnitude faster than C-centered radicals. The rate constant at 300 K for the unhindered molecule **3** was comparable to that for H-atom abstraction from Bu<sub>3</sub>SnH by *tert*-butoxyl, even though the BDE

(32) The simulation assumed isotropic behavior. However, at the low temperature of 155 K, restricted internal rotation in radical **14** is very probable because of the agglomeration of large groups. The nonideal agreement between some of the experimental line intensities with the simulated ones can probably be attributed to the selective line broadening resulting from this anisotropic motion.

(33) Walton, J. C.; McCarroll, A. J.; Chen, Q.; Carboni, B.; Nziengui, R. *J. Am. Chem. Soc.* **2000**, *122*, 5455–5463.

(34) Walton, J. C. *J. Chem. Soc., Perkin Trans. 2* **1998**, 603–605.

(35) Monot, J.; Makhoulouf Brahm, M.; Ueng, S.-H.; Robert, C.; Desage-El Murr, M.; Curran, D. P.; Malacria, M.; Fensterbank, L.; Lacôte, E. *Org. Lett.* **2009**, *11*, 4914–4917.



of the B–H bond is considerably greater. For preparative reductions with the new reagents, DTBP/UV and/or *tert*-butyl hyponitrite/heat will probably be the best initiator systems. The rate of H-atom abstraction was very sensitive to steric shielding around the BH<sub>3</sub> center, so the rate could easily be tuned. In the absence of an internal reaction partner, the NHC–boryl radicals dimerized to 1,2-bis-NHC–diboranes. The rate of this process was also strongly dependent on steric shielding but increased to the diffusion-controlled limit for sterically unhindered NHC–boryls.

Imidazole-based NHC–boryl radicals readily abstracted bromine atoms from alkyl, allyl, and benzyl bromides. Chlorine-atom abstraction was, however, much less efficient and only observed for the sterically unhindered radical **3**• reacting with allylic and benzylic chlorides. The radical **1b**•, lacking the quasi-aromatic structure, and the triazole-based radical **7**• were poorer bromine-atom acceptors, probably as a consequence of the lower unpaired spin on boron for these two species. An interesting elimination process was discovered for the NHC–borane **8** containing a bulky *thexyl* substituent at boron. The *tertiary* H atom of the *thexyl* group was selectively removed, yielding an unusual  $\beta$ -boron-containing alkyl radical. The latter rapidly underwent  $\beta$  scission of its B–C bond with production of an NHC–boryl radical and an alkene. In this respect, NHC–BH<sub>2</sub>–alkyl radicals resembled L<sub>n</sub>M–CH<sub>2</sub>CH<sub>2</sub>• radicals where M is an element from the second or subsequent row of the Periodic Table. The ease of this elimination suggests that addition reactions of NHC–boryl radicals with simple alkenes will be reversible at room temperature, so that hydroborations with NHC–boranes will only be achievable under special conditions.

## Experimental Section

**EPR Spectroscopy.** EPR spectra were obtained with a Bruker EMX 10/12 spectrometer fitted with a rectangular ER4122 SP resonant cavity and operating at 9.5 GHz with 100 kHz modulation. Usually stock solutions of the NHC–borane (2–15 mg) and DTBP (ca. 0.1 mL) in *tert*-butylbenzene (1.0 mL) were prepared and sonicated if necessary. An aliquot (0.2 mL), to which any additional reactant had been added, was placed in a 4 mm o.d. quartz tube, deaerated by bubbling nitrogen for 20 min, and photolyzed in the resonant cavity by unfiltered light from a 500 W super pressure mercury arc lamp. Solutions in cyclopropane were prepared on a

vacuum line by distilling in the cyclopropane, degassing with three freeze–pump–thaw cycles, and finally flame sealing the tubes. Most of the EPR spectra were recorded with 2.0 mW power, a 1.0 G<sub>pp</sub> modulation intensity, and a gain of ca. 10<sup>6</sup>. In all cases where spectra were obtained, hfs were assigned with the aid of computer simulations using the Bruker SimFonia and NIEHS Winsim2002 software packages. For kinetic measurements, precursor samples were used mainly in ‘single shot’ experiments; that is, new samples were prepared for each temperature and each concentration to minimize sample depletion effects. In a few cases second shot data were included. EPR signals were double integrated using the Bruker WinEPR software, and radical concentrations were calculated by reference to the double integral of the signal from a known concentration of the stable radical 2,2-diphenyl-1-picrylhydrazyl (DPPH) [ $1 \times 10^{-3}$  M in PhMe], run under identical conditions, as described previously.<sup>36</sup>

**Acknowledgment.** This work was supported by grants from the US National Science Foundation (CHE-0645998 to D.P.C.), Agence Nationale de la Recherche (ANR, BLAN0309 Radicaux Verts, and 08-CEXC-011-01, Borane), l'état et la région Ile-de-France (Chaire Blaise Pascal to D.P.C.), UPMC, CNRS, and IUF (M.M., L.F.). Technical assistance (MS, elemental analyses) was generously offered by FR 2769. A.S. thanks the University of Pittsburgh for a Graduate Excellence Fellowship. J.C.W. thanks EaStChem for financial support. We dedicate this paper to Professor Athelstan L. J. Beckwith for his 80th birthday.

**Supporting Information Available:** Experimental details of the preparations of imidazolium and triazolium salts and the corresponding boranes; NMR spectra of all new compounds; sample EPR spectra of NHC–boryl and related radicals; experimental and computed hfs of NHC–boryl radicals; computed torsion barrier in radical **3**•; kinetic data for NHC–boryl radical decays; details of photochemical reaction of NHC–BH<sub>2</sub>–*thexyl* **8** with DTBP; complete ref 19; DFT-optimized geometries and energies for the NHC–boryl radicals. This material is available free of charge via the Internet at <http://pubs.acs.org>.

JA909502Q

(36) Maillard, B.; Walton, J. C. *J. Chem. Soc., Perkin Trans. 2* **1985**, 443–450.